



Calculation method for wear of steel-bronze rolling-sliding contacts relating to worm gears

Philipp E. Schnetzer¹ · Josef Pellkofer¹ · Karsten Stahl¹

Received: 27 March 2023 / Accepted: 6 July 2023 / Published online: 8 August 2023
© The Author(s) 2023

Abstract

Worm gears are usually used in industrial applications with the material pairing of hard worm and softer worm wheel, where the failure mode wear often limits the service life. Up to now, extensive, costly and time-consuming component wear tests need to be carried out for each tribological pairing in order to calculate the amount of wear on worm wheels. Therefore, no practical and efficient experimental method is currently available to optimize material-lubricant pairings with respect to wear capacity for worm gear drives. For this reason, a model contact wear test was developed applying a twin-disk test rig. Based on this, the paper covers a new wear calculation method to characterize the wear behavior of steel-bronze rolling-sliding contacts regarding worm wheels. Therefore, the basics for the new calculation method for a model contact will be presented. Furthermore, the validation of the newly developed wear calculation method on the basis of test results of experimental investigations using the twin-disk test rig is addressed. Subsequently, results of the new wear calculation method are compared to results of the wear calculation method for worm wheels for individual tribosystems. Special focus will be given to similar trends in the calculated wear between the worm gear contact and the model contact. This new calculation method enables, in combination with wear tests on the twin-disk machine, efficient information on the wear behavior of worm gears and the development of optimized material-lubricant pairings concerning wear performance for worm gear drives.

Berechnungsmethode zur Beurteilung von Verschleiß bei Stahl-Bronze-Wälzpaarungen hinsichtlich Schneckengetrieben

Zusammenfassung

Schneckengetriebe werden in industriellen Anwendungen oftmals mit der Werkstoffpaarung harte Schnecke und weiches Schneckenrad eingesetzt, wobei die Lebensdauer häufig durch den Verschleiß am Schneckenrad begrenzt wird. Bisher sind für jede tribologische Paarung umfangreiche und zeitintensive Komponentenverschleißversuche am Schneckengetriebeprüfstand durchzuführen, um den Verschleiß an Schneckenrädern berechnen zu können. Zur effizienten Ermittlung des Verschleißverhaltens wurde deshalb eine Verschleißmethodik am Zweiseibenprüfstand entwickelt. Darauf aufbauend wird eine neue Verschleißberechnungsmethode zur Charakterisierung des Verschleißverhaltens von Stahl-Bronze-Wälzkontakten im Hinblick auf Schneckenrädern in Anlehnung an die ISO/TS 14521 [1] abgeleitet und in diesem Beitrag vorgestellt. Dazu wird der Berechnungsablauf präsentiert und eine Validierung anhand von Versuchsergebnissen aus experimentellen Untersuchungen am Zweiseibenprüfstand vorgenommen. Anschließend werden die Ergebnisse der neuen Verschleißberechnungsmethode mit den Ergebnissen der Verschleißberechnungsmethode für Schneckengetriebe nach ISO/TS 14521 [1] für unterschiedliche Tribosysteme verglichen.

✉ Philipp E. Schnetzer
philipp.schnetzer@tum.de

¹ Gear Research Center (FZG), Department of Mechanical Engineering, TUM School of Engineering and Design, Technical University of Munich, Garching, Germany

1 Introduction

Worm gear drives are a type of gearbox that are suitable for certain applications due to the possibility of high transmission ratios in one stage, a compact design, the ability to self-lock, and low-noise running behavior. Currently, indus-

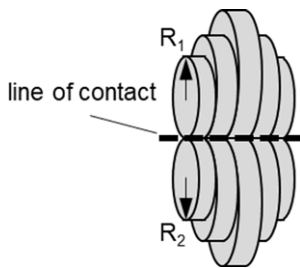


Fig. 1 Abstracted tooth contact using rollers acc. to [2]

trial applications mostly use pairings of a hard worm (case-hardened steel/tempered steel) and a softer worm wheel (bronze/cast iron). Due to relatively large sliding portions during the rolling-sliding of the worm gearing, wear occurs in small gear box sizes, which manifests itself predominantly on the bronze worm wheel and can limit the service life or the function of the gear box.

Due to the complex loading conditions and the lack of knowledge about the influence of the material-lubricant pairing the estimation and calculation of the wear load capacity is complicated. Therefore, extensive experimental component tests on a worm gear test rig are necessary in order to be able to predict the wear load capacity for a material-lubricant pairing. The wear methodology developed on the twin-disk test rig, in combination with the new calculation method presented in this paper and based on two disks, should lead more quickly to knowledge about the abrasive wear behavior of steel-bronze rolling-sliding contacts such as those used in worm gear drives.

The analogy by means of two disks was already used by Weber and Niemann [2]. They abstract the worm gear contact along the line of contact into individual sections with simplified rollers, as shown in Fig. 1.

Based on this, Wilkesmann [3] developed a software program for the calculation of load carrying capacity parameters by means of substitute rollers. Based on Wilkesmann, Predki [4] continues the analytical contact calculation on simplified rollers and defines dimensionless characteristic parameters, which represent a basis for the load capacity calculation according to ISO/TS 14521 [1]. The wear calculation for worm gears according to Neupert [5] contained in ISO/TS 14521 [1] is consequently based on the description of the worm gear tooth contact by means of substitute rollers. It is therefore an obvious step to determine wear parameters on a twin-disk contact as presented in this paper.

2 State of the art

Numerous experimental investigations have been performed on tribometers for the material pairings steel/steel and steel/plastic. For the material pairing steel/bronze, there are significantly less investigations in literature. Oehler et al. [6] investigate the friction of steel-bronze contacts on a twin-

disk rest rig under boundary and mixed lubrication to analyze the local coefficient of friction of a worm gear box. Oetue [7] studies the relationship between the initiation of pitting failure and Hertzian pressure with steel-bronze pairing on a disk-roller test rig and transfers the results to worm gears. The authors are not aware of any paper in which systematic wear investigations have been carried out on the twin-disk test rig for steel-bronze pairing. Therefore, the focus of the following part is on wear investigations of worm gears.

2.1 Wear investigations of worm gears

Steel-bronze rolling-sliding contacts are found in applications such as worm gears, hence the focus on worm gear drives in the following. Due to the sliding conditions of worm gear drives and the usual hard-soft pairings, wear cannot be completely avoided. FZG/Heilemann [8] analyzes the effects of different worm profiles according to Niemann and Winter [9] on wear behavior. ZC gears (according to [9]) exhibit lower operating wear in the usual application range compared to ZI gears.

Nass [10] investigates the effects of bronze composition on the resulting material structure and load carrying capacity of the worm wheel. The investigations indicate that a bronze structure with small grain sizes, high nickel content of 4% and phosphorus content less than 0.1% positively affects the wear carrying capacity of a worm gear. Building on Nass, Sievers [11, 12] explores the effects of casting parameters in centrifugal casting on structure formation and on the wear carrying capacity of worm gears. Sievers presents an approach to characterize the bronze structure of worm gears with respect to wear resistance.

In experimental investigations, FZG/Weisel [13] establishes that worm gear drives with small center distances exhibit comparatively high wear rates compared to large sizes due to the lower circumferential speeds and poorer lubricant film formation.

2.2 Wear calculation of worm gears

According to Meng and Ludema [14], more than 300 different methods for calculating friction and wear processes exist in the literature. The currently available calculation methods usually include empirically determined factors that capture the complex interaction between material and lubricant.

Based on the work of FZG/Weisel [13], FZG/Sigmund [15] developed a wear calculation method for worm gear drives with incomplete contact pattern. This method can be used to calculate operational wear during the development of the contact pattern in the running-in.

Based on Archard equation [16] and considering lubrication, a wear model for worm gears is presented by Jbily

et al. [17]. The validation shows that higher wear is determined with the calculation compared to the experimental results.

Similarly, Sharif et al. [18] present a wear calculation for worm gear drives based on Archard equation [16] to determine the calculated wear per meshing cycle. The model provides for an individual adaptation to the considered gearing by adjusting the lubricant film thickness, taking into account the wear pattern observed in experimental investigations.

Daubach et al. [19] present a wear simulation that is transient and therefore able to predict the evolution of the contact pattern over time. The simulation includes a tooth contact analysis and a tribological approach to calculate the tooth friction coefficient and further the wear.

Based on the wear model according to Archard [16], FZG/Neupert [5] develops a wear calculation for worm gears using a wear intensity J_w and thus creates the basis for the wear calculation according to ISO/TS 14521 [1]. For this purpose, he introduces local parameters such as the minimum mean lubricant film thickness $h_{min m}$, the mean sliding path s_{gm} and the mean wear path s_{wm} on the basis of dimensionless characteristic parameters according to Predki [4]. This wear calculation is widely used and forms the basis for the calculation of wear for worm gears in this paper.

FZG/Norgauer [20] investigates the wear behavior of small worm gears and shows that the wear calculation according to ISO/TS 14521 [1] is applicable for small gear sizes.

2.3 Conclusion from the state of the art and problem formulation

For a most accurate possible wear calculation for worm gears, as for example according to ISO/TS 14521 [1], characteristic wear values need to be determined experimentally for the selected material-lubricant pairing. For this purpose, wear tests are currently carried out on worm gear test rigs, although these tests are very time-consuming and subject to a high degree of scatter [20]. Therefore, no practical and efficient experimental method is currently available to optimize material-lubricant pairings with respect to wear capacity for worm gear drives.

Furthermore, an efficient and low scatter experimental methodology and wear calculation are desirable to develop optimized material-lubricant pairings with respect to wear performance for worm gear drives.

3 Experimental investigations

3.1 Twin-disk test rig and disks

The experimental wear tests on the model test rig are carried out on the FZG twin-disk test rig, which is shown schematically in Fig. 2. The following description and formulations are mainly based on Ebner et al. [21]. The test rig consists of two disks, which represent the test specimens and are driven independently of each other by means of an electric motor. Thus, the variable speed setting of the disks allows different sum speeds and sliding speeds in the disk contact. A pneumatic cylinder is used to continuously apply the normal force to the disks, pressing the flat running tracks of the disks together. The upper disk is rotatably mounted in a skid. The lower disk is rotatably mounted on a skid, which is horizontally movable and supported by spring bands on a load cell. This allows the frictional force, which will not be discussed in this article, to be measured.

As a further measured parameter, the bulk temperature of the steel disk is recorded with a Pt 100 sensor. A Mettler Toledo XPR2004SC balance is used to determine the wear rate. The manufacturer gives typical values for linearity deviation as 0.5 mg and for repeatability as 0.3 mg with a readability of 0.1 mg.

The test disks show an outside diameter at the running surface of 80 mm and are cylindrical, so there is line contact in the contact area of the disks, as is the case with worm gear drives. Each time the disks are removed and installed, the contact pattern is checked by means of a contact pattern sheet, thus preventing edge contact. The width of the bronze disk is 10 mm and the width of the steel disk is 12 mm. The measured surface roughnesses are in the range of $Ra \approx 0.8...1.0 \mu\text{m}$ for the bronze test disks and $Ra \approx 0.4...0.6 \mu\text{m}$ for the steel test disks. The measurement is performed in the width direction, as the disks are processed in the circumferential direction.

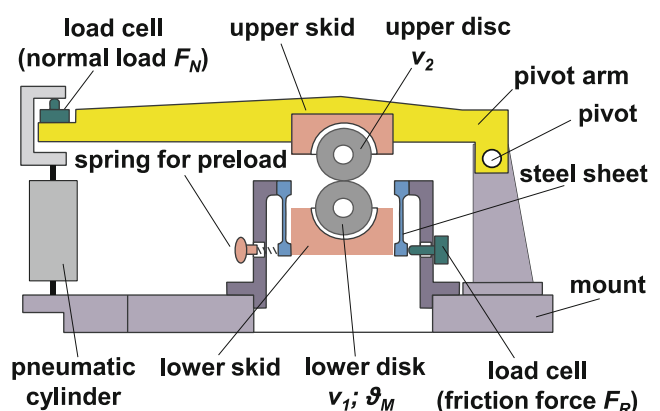


Fig. 2 FZG twin-disk test rig [22]

The tests are performed with injection lubrication at an oil volume flow of $Q_{oil} = 1.41/\text{min}$ at an oil injection temperature of $\vartheta_E = 100^\circ\text{C}$. With the higher oil injection temperature compared to the injection temperature of 80°C for the worm gear tests, even more unfavorable lubrication conditions can be achieved. Due to the test rig design, it is not possible to reduce the minimum sum velocity—which has a decisive influence on the lubricant film formation—to below 0.5 m/s . The influence of the higher injection temperature on the test results is compensated by the calculation method presented, as is the case with the wear calculation for worm gear drives in accordance to ISO TR 14521.

3.2 Worm gear test rig and gears

The experimental component wear tests are carried out on a worm gear test rig. The following description and formulations are mainly based on Sigmund [23]. Figure 3 shows the schematic design of the test rig based on the motor-generator principle. Here, the electric motor (1) provides the input torque T_1 on the input side.

The shaft of the electric motor is connected to the worm shaft of the test gear box (2). The test gearbox converts the input speed n_1 and the input torque T_1 according to the gear ratio. The worm gear shaft on the output side is connected to a reduction gear box (3). This converts speed and torque for the generator (4).

The input torque T_1 and output torque T_2 are measured using torque measuring shafts directly in front and behind the test gear box. The bulk temperature of the worm wheel is measured using a NiCr-Ni sensor. The amount of wear is determined on a Mettler Toledo XPR5003S balance. The manufacturer specifies typical values for the linearity devi-

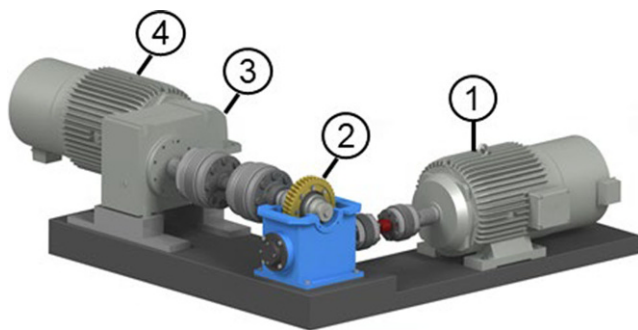


Fig. 3 Worm gear test rig center distance $a = 100\text{ mm}$

Table 2 Oil data

Oil designation	Oil 1-220	Oil 1-460	Oil 1-680	Oil 2	Oil 3	Oil 3_wAW
Density ρ at 15°C / kg/m^3	1060	1074	1075	1075	1055	1055
Kin. viscosity ν_{40} / mm^2/s	220	460	680	320	460	460
Kin. viscosity ν_{100} / mm^2/s	40	71	110	57	75	75

Table 1 Basic worm gear geometry data

Standard reference gear according to ISO/TS 14521 [1]			
Center distance	a	mm	100
Normal pressure angle	α_n	$^\circ$	20
Teeth ratio	z_1/z_2	–	41/2
Normal module	m_n	mm	4
Worm reference diameter	d_{m1T}	mm	36
Worm wheel reference diameter	d_{m2T}	mm	164
Face width	b_{2H}	mm	30
Reference lead angle of worm	γ_{m1}	$^\circ$	12.5

ation as 2 mg and for the repeatability as 1 mg with a readability of 1 mg .

The main geometrical data of the worm gears used can be seen in Table 1.

The surface roughnesses are measured in the middle of the tooth flank from the tooth root in the direction of the tooth tip. In the new condition roughnesses of $Ra \approx 0.4\text{--}0.6\text{ }\mu\text{m}$ for the worm shafts and $Ra \approx 0.5\text{--}0.8\text{ }\mu\text{m}$ for the worm wheels are measured. Thus, the roughnesses of the gears are in a comparable range to the roughnesses of the test disks.

The tests are performed with injection lubrication at an oil volume flow of $Q_{oil} = 71/\text{min}$ at an oil injection temperature of $\vartheta_E = 80^\circ\text{C}$.

3.3 Materials and oils

The parameters of the oils used, which are necessary for the calculation, are shown in Table 2. All oils are based on polyglycols. Oil 1 is available in three different viscosities. Oil 3_wAW contains no explicit anti wear additive and is otherwise the same than oil 3.

The same materials are used for the disk tests and the worm gear tests:

- 16MnCr5 case hardened and grounded: lower disk and worm
- GC-CuSn12Ni2: upper disk and worm wheel

4 Experimental results

The following experimental results are only briefly presented, but not explained in detail, as they are only used for

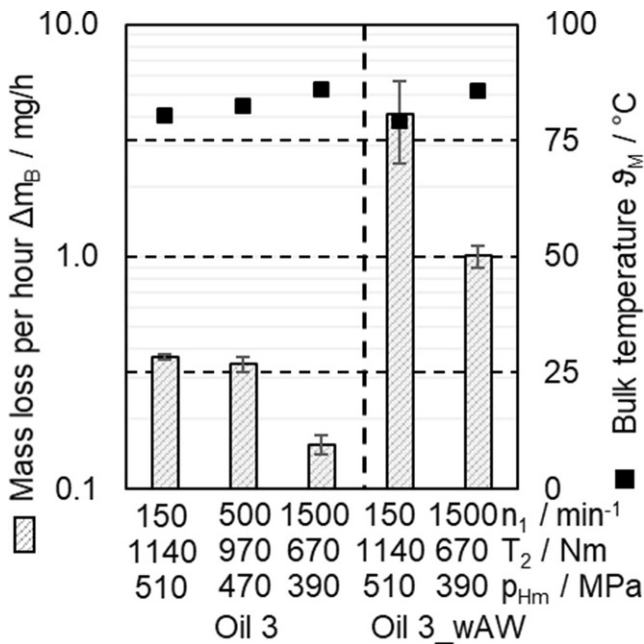


Fig. 4 Experimental results on the worm gear test rig for oil 3 and oil 3_wAW contains two tests each

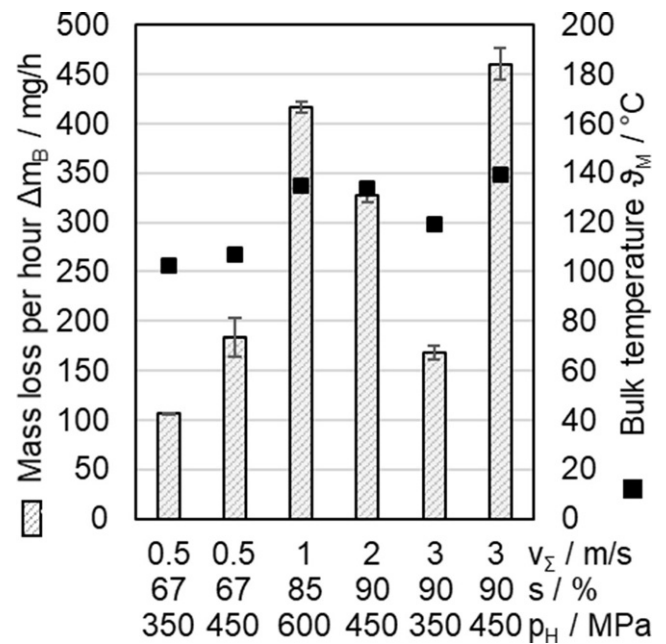


Fig. 6 Experimental results on the twin-disk test rig for oil 2 contains two tests each

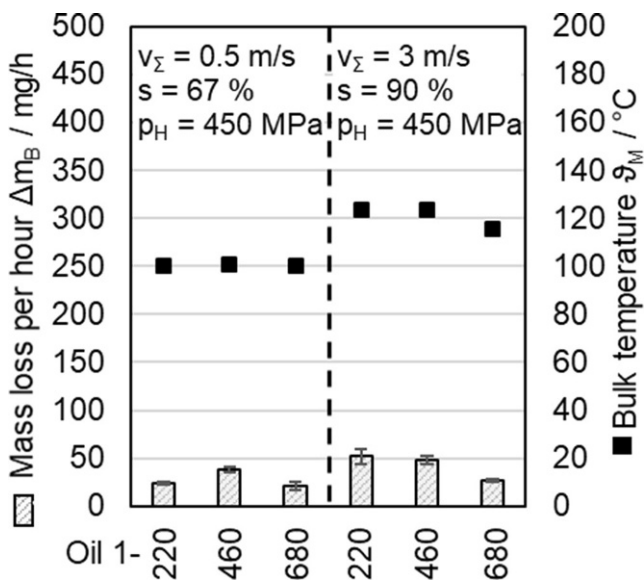


Fig. 5 Experimental results on the twin-disk test rig for different viscosities of oil 1 contains three tests each

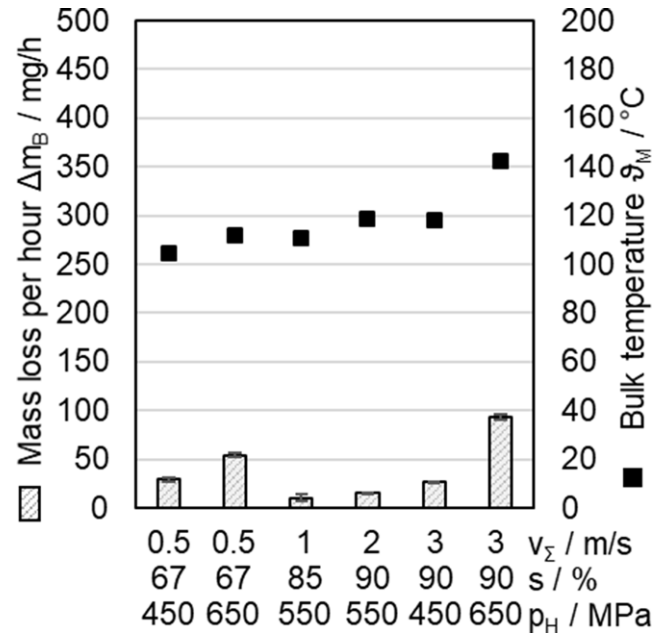


Fig. 7 Experimental results on the twin-disk test rig for oil 3 contains two tests each

the validation of the calculation method. In the diagrams, the number of tests for one operating condition is noted. The scatter of the results is indicated with error bars, although for the temperatures this is so low that no error bars are visible. A running-in of the disks and gears is performed before the wear measurements. The results of the experimental wear tests on the worm gear test rig are structured by the operating conditions such as input speed n_1 and the output torque T_2 and are shown in Fig. 4 for oil 3

and oil 3_wAW. The evaluation is carried out according to ISO/TS 14521 [1].

The results of the experimental wear tests on the twin-disk test rig are structured by the operating conditions such as sum velocity v_Σ , the slip ratio $s (= 100\% \cdot (v_1 - v_2) / v_1)$ and the Hertzian pressure p_H and are shown for oil 1 in Fig. 5, for oil 2 in Fig. 6, for oil 3 in Fig. 7 and for oil 3_wAW

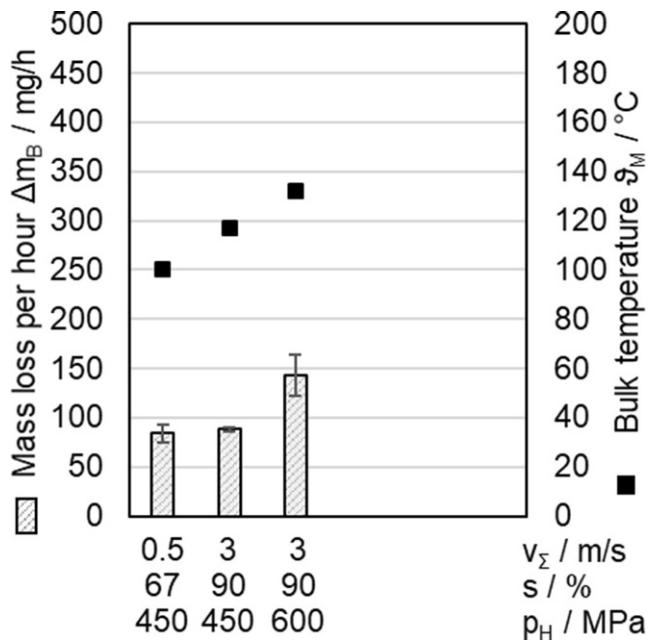


Fig. 8 Experimental results on the twin-disk test rig for oil 3_wAW contains three tests each

in Fig. 8. The evaluation is carried out in Sect. 5 using the presented calculation method.

5 New calculation method for wear of rolling-sliding contacts

The newly developed calculation method for calculating abrasive wear for the twin-disk contact for the steel-bronze-pairing is derived from the procedure for worm gear drives according to ISO/TS 14521 [1]. In this process, the abrasive wear of the bronze disk is defined as evenly distributed over the width of the disk and normal to the running track in the direction of the radius. The wear is described as the running track loss δ_w and is calculated by means of the wear path s_w and the so-called wear intensity J_w as follows:

$$\delta_w = J_w(K_w) \cdot s_w \quad (1)$$

The wear path s_w describes the wear distance covered over the running time Δt and is defined with the sliding speed v_g as follows:

$$s_w = v_g \cdot \Delta t \quad (2)$$

The sliding speed v_g is defined from the tangential velocities of the running track of the disks v_1 and v_2 as follows:

$$v_g = v_1 - v_2 \quad (3)$$

The wear intensity J_w is a de-dimensioned parameter and is determined experimentally on the twin-disk test rig for each material-lubricant pairing depending on the lubrication conditions. The lubrication conditions are incorporated in the lubricant film thickness parameter K_w , which can be calculated. Thus, for each material-lubricant pairing investigated, the function between the wear intensity J_w and the lubricant film thickness parameter K_w must be derived to calculate wear. To derive the function, the total material loss of the bronze disk for a single lubrication condition (i) is determined on the twin-disk test rig. For this lubrication condition (i), the running track loss $\delta_{w,i}$ is calculated with the total material loss $m_{ges,i}$, the running track area A_L and the density ρ of the bronze disk as follows:

$$\delta_{w,i} = \frac{m_{ges,i}}{A_L \cdot \rho} \quad (4)$$

The running track area A_L is assumed to be constant during the test run and is defined from the diameter of curvature D_2 of the bronze disk and the width b of the running track.

$$A_L = D_2 \cdot \pi \cdot b \quad (5)$$

Using the experimental determined running track loss $\delta_{w,i}(K_{w,i})$ for a lubrication condition (i) and the wear path $s_{w,i}$, the wear intensity $J_{w,i}$ is calculated according to ISO/TS 14521 [1] as follows:

$$J_{w,i}(K_{w,i}) = \frac{\delta_{w,i}(K_{w,i})}{s_{w,i}} \quad (6)$$

If the wear intensity $J_{w,i}$ is determined for at least two lubrication conditions (i), a function between wear intensity J_w and lubricant film thickness parameter K_w can be specified by means of regression calculation for a material-lubricant pairing. In Sect. 6 this is presented as an example for two material-lubricant pairings.

To describe the lubrication condition, the calculation of the lubricant film thickness parameter K_w is presented in the following. The calculation is based on the minimum lubricant film thickness h_{min} and is modified with the lubricant structure factor W_s and the pressure factor W_H according to ISO/TS 14521 [1]:

$$K_w = h_{min} \cdot W_s \cdot W_H \quad (7)$$

The lubricant structure factor W_s takes into account the different viscosity behavior of polyglycols and polyalphaolefins with regard to wear behavior compared to mineral oils [5]. The pressure factor W_H considers the influence of the contact pressure on the wear behavior [24].

The choice of the factors W_S and W_H is discussed following the calculation presentation. The minimum lubricant film thickness is calculated according to Dowson and Higginson [25] with the dimensionless characteristic parameters for the line contact G , U and W to:

$$h_{\min} = 2.65 \cdot G^{0.54} \cdot U^{0.7} \cdot W^{-0.13} \cdot R \quad (8)$$

The material parameter is defined according to Dowson and Higginson [25] as follows:

$$G = \alpha_p \cdot E' \quad (9)$$

The lubricant film formation is significantly determined by the conditions in the inlet of the elastohydrodynamic lubrication (EHL). Therefore, Simon [26] proposes the bulk temperature and the pressure $p=200$ MPa as conditions for the calculation of the pressure viscosity exponent $\alpha_p(\vartheta_M, p)$. The lubricant film thicknesses calculated with these conditions show good correspondence with measurements at the FZG twin-disk test rig [26]. Accordingly, these conditions are used for the lubricant film thickness calculations of the EHL contact. The calculation of the pressure viscosity exponent α_p is carried out for the disk model according to the Modul equation [27]:

$$\alpha_p(\vartheta_M, p) = \frac{1}{a_1 + a_2 \cdot \vartheta_M + (b_1 + b_2 \cdot \vartheta_M) \cdot p} \quad (10)$$

As coefficients for the pressure viscosity exponent, the values determined for the commercial oil GH 6-460 from the investigations on FVA 729 II [28] are applied as an approximation for the oils used, since this shows comparable properties to the oils investigated. The characteristic speed value U is calculated according to Dowson and Higginson [25] as follows:

$$U = \frac{\eta(T_M) \cdot v_\Sigma}{E' \cdot R} \quad (11)$$

The dynamic viscosity η is calculated according to ISO/TS 14521 [1] for the wear calculation as a function of the bulk temperature and the ambient pressure. For comparability of the disk and worm wear calculation, the dynamic viscosity η in the inlet of the EHL contact is determined with the same conditions according to DIN 1342-2 [29].

$$\eta(T_M) = \nu(T_M) \cdot \varrho \quad (12)$$

The kinematic viscosity ν is determined as a function of temperature and the directional parameter m according to DIN 51563 [30].

$$\nu(T_M) = \exp(\exp(m \cdot (\lg(T_1) - \lg(T_M)) + \lg(\lg(\nu_1 + 0.8)))) - 0.8 \quad (13)$$

$$m = \frac{\lg(\lg(\nu_1 + 0.8)) - \lg(\lg(\nu_2 + 0.8))}{\lg(T_2) - \lg(T_1)} \quad (14)$$

The sum velocity v_Σ is defined by the tangential velocities of the running track of the disks and serves as entrainment speed for the EHL film formation.

$$v_\Sigma = v_1 + v_2 \quad (15)$$

The load parameter W is calculated according to Dowson and Higginson [25] as follows:

$$W = 2 \cdot \pi \cdot \left(\frac{p_H}{E'}\right)^2 \quad (16)$$

For line contact, the Hertzian pressure p_H is calculated with the reduced Young's modulus E' and the reduced radius of curvature R according to Niemann and Winter [31] as follows:

$$p_H = \sqrt{\frac{F_N \cdot E'}{2 \cdot \pi \cdot R \cdot l_{\text{eff}}}} \quad (17)$$

$$E' = \frac{2}{\frac{(1-\nu_1^2)}{E_1} + \frac{(1-\nu_2^2)}{E_2}} \quad (18)$$

The reduced radius of curvature R is used to describe the geometry of the investigated disk contact and is calculated according to Niemann and Winter [31]:

$$R = \frac{D_1 \cdot D_2}{2 \cdot (D_1 + D_2)} \quad (19)$$

According to ISO/TS 14521 [1], the lubricant film thickness parameter K_W is composed of the minimum lubricant film thickness h_{\min} and the factors W_S and W_H . The impact of the lubricant structure factor W_S introduced by Neupert [5] and the pressure factor W_H defined by Steingröver [24] on the developed disk wear calculation are studied below. For this purpose, experimental investigations are carried out with different contact pressures for several material-lubricant combinations.

The results are plotted in Fig. 9 in the form of wear intensity versus minimum lubricant film thickness h_{\min} , as is

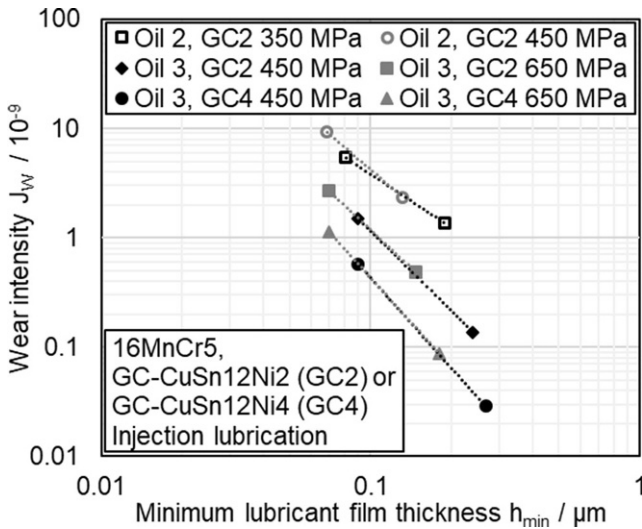


Fig. 9 Influence of different contact pressures for various material-lubrication pairings: wear intensity over minimum lubricant film thickness

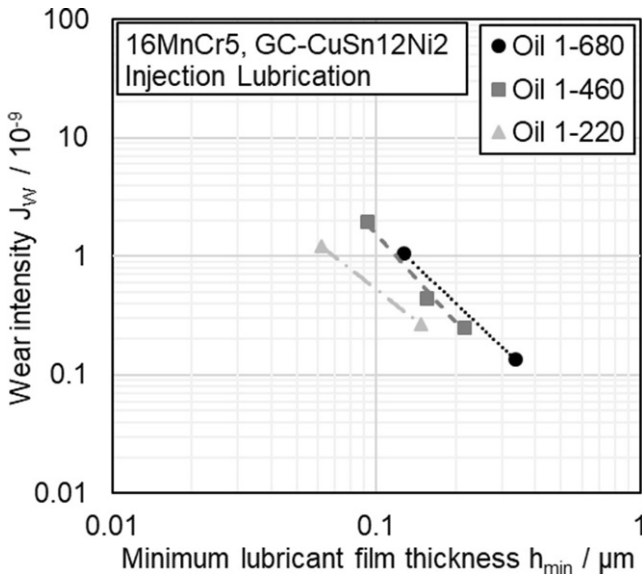


Fig. 10 Influence of different viscosities: wear intensity over minimum lubricant film thickness

also usual for worm gear drives according to ISO/TS 14521 [1]. It can be seen that the wear intensity and thus the wear on the bronze disk increases with decreasing minimum lubricant film thickness (for example, for a decreasing sum speed). For the different contact pressures investigated, approximately congruent wear intensity lines are evident for the same material-lubricant pairing. Therefore, no additional influence of the contact pressure on the developed wear calculation is to be assumed, for which reason the pressure factor for the disk wear calculation is set to $W_H = 1$.

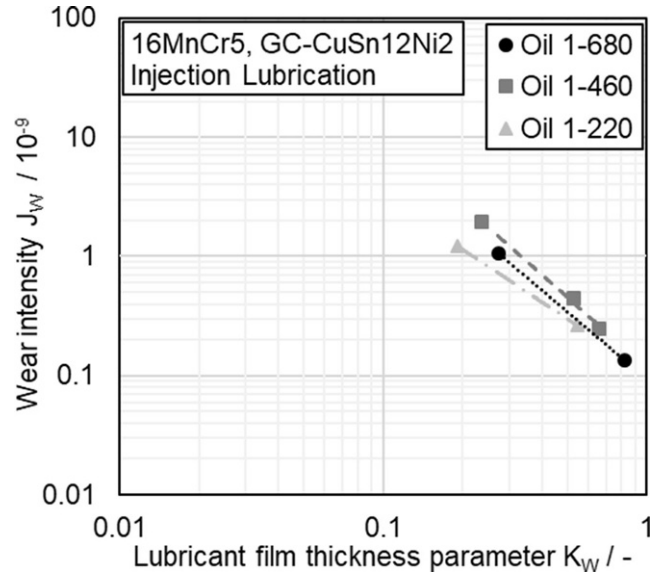


Fig. 11 Influence of different viscosities: wear intensity over lubricant film thickness parameter

To analyze the lubricant structure factor W_S , experimental investigations are carried out with three different viscosities of the polyglycol-based oil 1.

In Fig. 10 the wear intensities are plotted against the minimum lubricant film thickness h_{min} . The wear intensities of the oils with different viscosities diverge. Consequently, the calculation approach does not adequately estimate the effect of viscosity on the lubricant film thickness h_{min} for the polyglycol-based oil. The same effect is observed by Neupert [5] for the wear calculation for worm gears when polyglycols are used, and therefore the lubricant structure factor W_S is introduced. For the present calculation approach, the lubricant structure factor W_S is determined as follows for polyglycols and polyalphaolefins analogous to ISO/TS 14521 [1]:

$$W_S = \frac{1}{\eta(T_M)^{0.35}} \cdot \tag{20}$$

The wear intensities considering the lubricant structure factor W_S are shown in Fig. 11. The individual wear intensity lines for the lubricants with different viscosities are now closer together, with a simultaneous shift in the wear intensities towards more favorable lubrication conditions. A comparable characteristic is observed by Neupert [5] for the introduced lubricant structure factor W_S for worm gears.

6 Application of the calculation method

The validation of the presented calculation method is carried out using two oils for several operating conditions,

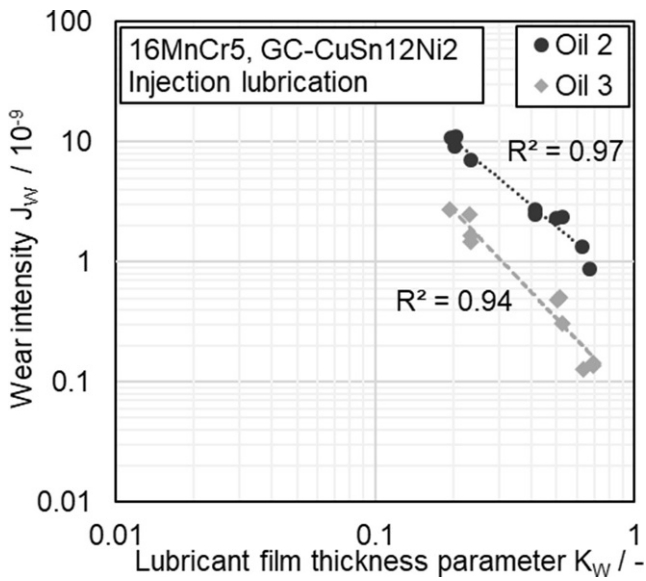


Fig. 12 Coefficient of determination for the calculation method

as shown in Fig. 12. The wear tests are subject to scatter. To describe the correlation between wear intensity J_W and lubricant film thickness parameter K_W , a regression calculation is therefore used to determine a compensation curve. This is represented in the double logarithmic diagram as an averaging straight line. For Oil 2 and Oil 3 the calculated functions between wear intensity J_W and lubricant film thickness parameter K_W are as follows:

$$J_{W,Oil2} = 5.7 \cdot 10^{-10} \cdot K_W^{-1.81}, \tag{21}$$

$$J_{W,Oil3} = 7 \cdot 10^{-11} \cdot K_W^{-2.27}. \tag{22}$$

The coefficient of determination is used to assess the quality of the regression. With $R^2=0.94\dots0.97$, these values are in a high range and indicate a good fit for the determined wear intensities of both lubricants. In conclusion, it can be stated that the derived disk wear calculation suitably describes the wear behavior for the operating conditions and lubricants investigated.

7 Comparison of wear behavior between the model contact and the worm gear contact

In the following, the established worm wear calculation method according to ISO/TS 14521 [1] is compared with the wear calculation presented within this paper for the model rolling-sliding contact (disk wear calculation) for two lubricants in Fig. 13. For both calculation approaches, the wear intensity for “Oil 3_wAW” is above that for “Oil 3”. Likewise, the wear intensities for both oils are

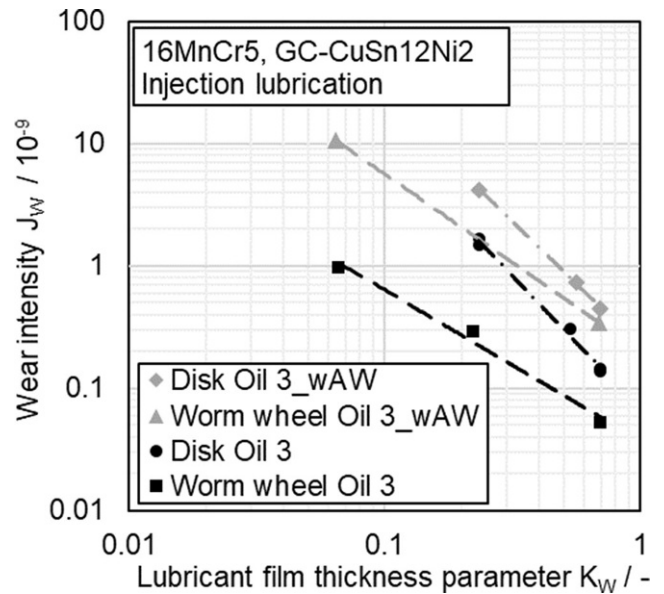


Fig. 13 Comparison of wear intensity between model contact and worm gear contact

shifted nearly in parallel for both calculation approaches. A direct comparison of the wear lines shows a greater gradient and a wear intensity shifted to higher wear rates for the disk wear methodology compared to the worm gear method. Thus, the disk wear calculation shows the same tendencies as the worm wear calculation. This allows conclusions to be drawn about the wear behavior in the worm tooth contact. In the future, this offers the potential to develop targeted material-lubrication pairings for low wear on worm gear drives.

8 Conclusion

Overall, it can be shown that the wear behavior for a steel-bronze pairing can be described with the derived wear calculation for bronze disks based on the test methodology on the twin-disk test rig. Furthermore, similar trends in wear behavior can be observed between worm gears and disks. Consequently, conclusions on the wear behavior of worm gear drives are possible with the derived wear calculation. The calculation method presented in combination with the test method on the twin-disk test rig therefore offers an efficient way to predict the wear behavior of steel-bronze rolling-sliding pairings, as in the case of worm gear drives, for different material-lubricant pairings. This results in the possibility of designing targeted material-lubrication pairings for low wear on worm gear drives in the future.

Table 3 Symbols

A_L	mm ²	Running track area
a	mm	Center distance
a_1	N/m ²	Lubricant parameter
a_2	N/(m ² °C)	Lubricant parameter
b_1	–	Lubricant parameter
b_2	1/°C	Lubricant parameter
D	mm	Diameter of curvature
E	N/mm ²	Young's modulus
E'	N/mm ²	Reduced Young's modulus
F_N	N	Normal-load
G	–	Material parameter
h_{\min}	μm	Minimum film thickness
J_W	–	Wear intensity
K_W	–	Lubricant film thickness par.
l_{eff}	mm	Effective width
m	–	Direction parameter
m_{ges}	mg	Total material loss
p	N/m ²	Pressure in contact area
p_H	MPa	Hertzian pressure
R	mm	Reduced radius of curvature
s_W	mm	Wear path
T	K	Test temperature
T_M	K	Bulk temperature
Δt	s	Running time
U	–	Velocity parameter
v	m/s	Velocity
v_g	m/s	Sliding velocity
v_{Σ}	m/s	Sum velocity
W	–	Load parameter
W_H	–	Pressure factor
W_S	–	Lubricant structure factor
α_p	m ² /N	Pressure viscosity factor
δ_W	mm	Running track loss
η	Ns/m ²	Dynamic viscosity
ϑ_M	°C	Bulk temperature
ν	–	Poisson ratio
ν	m ² /s	Kinematic viscosity
ρ	kg/m ³	Density
Indices		
1	–	Lower disk/test temperature 1
2	–	Upper disk/test temperature 2

9 Symbols

The symbols are shown in Table 3.

Acknowledgements The presented results are based on the research project FVA 849 I/IGF no. 20108 N1 undertaken by the Research Association for Drive Technology e. V. (FVA) and supported partly by the FVA and through the German Federation of Industrial Research Associations e. V. (AiF) in the framework of the Industrial Collective Research (IGF) program by the Federal Ministry for Economic Affairs

and Climate Action (BMWK) based on a decision taken by the German Bundestag. The authors would like to thank for the sponsorship and support received from the FVA and the AiF as well as from the members of the project committee.

Funding Open Access funding enabled and organized by Projekt DEAL.

Conflict of interest P. E. Schnetzer, J. Pellkofer and K. Stahl declare that they have no competing interests.

Open Access This article is licensed under a Creative Commons Attribution 4.0 International License, which permits use, sharing, adaptation, distribution and reproduction in any medium or format, as long as you give appropriate credit to the original author(s) and the source, provide a link to the Creative Commons licence, and indicate if changes were made. The images or other third party material in this article are included in the article's Creative Commons licence, unless indicated otherwise in a credit line to the material. If material is not included in the article's Creative Commons licence and your intended use is not permitted by statutory regulation or exceeds the permitted use, you will need to obtain permission directly from the copyright holder. To view a copy of this licence, visit <http://creativecommons.org/licenses/by/4.0/>.

References

- ISO/TS 14521:2020-04 (2020) Gears—Calculation of load capacity of worm gears
- Niemann G, Weber C (1942) Schneckengetriebe mit flüssiger Reibung. VDI-Forschungsheft, vol 312
- Wilkesmann H (1974) Berechnung von Schneckengetrieben mit unterschiedlichen Zahnprofilformen (Dissertation, Technische Universität München)
- Predki W (1982) Hertzische Drücke, Schmierpalthehöhen und Wirkungsgrade von Schneckengetrieben (Dissertation, Ruhr-Universität Bochum)
- Neupert K (1990) Verschleißtragfähigkeit und Wirkungsgrad von Zylinder-Schneckengetrieben (Dissertation, Technische Universität München)
- Oehler M, Sauer B, Magyar B (2019) Efficiency of worm gear drives under transient operating conditions. *J Tribol* 141(12). <https://doi.org/10.1115/1.4044655>
- Octue M (1989) A New Method of Designing Worm Gears. *Gear Technology* 1989(July/August):20–42
- Heilemann J (2005) Tragfähigkeit und Wirkungsgrad bei unterschiedlichen Schnecken-Zahnflankenformen unter Berücksichtigung der Oberflächenhärte und Härtetiefe (Dissertation, Technische Universität München)
- Niemann G, Winter H (1986) Schraubrad-, Kegelrad-, Schnecken-, Ketten-, Riemen-, Reibradgetriebe, Kupplungen, Bremsen, Freiläufe. *Maschinenelemente*, vol 3. Springer, Berlin, Heidelberg, New York, Tokyo
- Nass U (1995) Tragfähigkeitssteigerung von Schneckengetrieben durch Optimierung der Schneckenradbronze (Dissertation, Ruhr-Universität Bochum)
- Sievers B (2012) Verschleiß- und Grübchentragfähigkeit von Bronze-Schneckenrädern in Abhängigkeit von ihrer Gefügeausbildung (Dissertation, Ruhr-Universität Bochum)
- Sievers B, Predki W (2013) Load bearing capacity of bronze worm wheels depending on their material characteristics. In: *Tagungsband International Conference on Gears*. VDI-Berichte, vol 2199-2, pp 1209–1220
- Weisel C (2009) Schneckengetriebe mit lokal begrenztem Tragbild (Dissertation, Technische Universität München)

14. Meng HC, Ludema KC (1995) Wear models and predictive equations: their form and content. *Wear* 181–183(2):443–457
15. Sigmund W (2015) Simulating the wear behaviour of worm gears with local contact pattern. In: *Proceedings of the international conference on gears in Munich*, vol 2015, pp 799–809
16. Archard JF (1953) Contact and rubbing of flat surfaces. *J Appl Phys* 24(8):981–988
17. Jbily D, Guingand M, Vaujany J-P (2016) A wear model for worm gear. *Proc Inst Mech Eng C: J Mech Eng Sci* 230(7–8):1290–1302
18. Sharif KJ, Evans HP, Snidle RW (2006) Prediction of the wear pattern in worm gears. *Wear* 261(5–6):666–673
19. Daubach K, Oehler M, Sauer B (2022) Wear simulation of worm gears based on an energetic approach. *Eng Res* 86(3):367–377
20. Norgauer P (2021) Verschleißverhalten von modernen Schneckenverzahnungen (Dissertation, Technische Universität München)
21. Ebner M, Ziegltrum A, Lohner T, Michaelis K, Stahl K (2018) Measurement of EHL temperature by thin film sensors—thermal insulation effects. *Tribol Int* 149. <https://doi.org/10.1016/j.triboint.2018.12.015>
22. Ebner M, Lohner T, Michaelis K, Stemplinger J-P, Höhn B-R, Stahl K (2016) Self-lubricated elastohydrodynamic (EHL) contacts with oil-impregnated sintered materials. In: *TAE Esslingen 20th international colloquium: tribology—industrial and automotive lubrication*
23. Sigmund W (2015) Untersuchung und Simulation des Verschleißverhaltens von Schneckengetrieben mit unvollständigem Tragbild (Dissertation, Technische Universität München)
24. Steingröver K (1993) Untersuchungen zu Verschleiß, Verlustgrad und Fressen bei Zylinder-Schneckengetrieben (Dissertation, Technische Universität München)
25. Dowson D, Higginson GR (1966) *Elasto-hydrodynamic lubrication—the fundamentals of roller and gear lubrication*. Pergamon Press, Oxford
26. Simon M (1984) Messung von elasto-hydrodynamischen Parametern und ihre Auswirkung auf die Grübchentragefähigkeit vergüteter Scheiben und Zahnräder (Dissertation, Technische Universität München)
27. Gold PW, Schmidt A, Loos J, Aßmann C (2001) Viskosität-Druck-Koeffizienten von mineralischen und synthetischen Schmierölen. *Tribol Schmierungstech* 47. 40–48
28. Oehler M, Werner M, Magyar B (2020) Ganzheitliche Wirkungsgradoptimierung von Schneckengetrieben. FVA-Nr. 729 II, vol 1384. *Forschungsvereinigung Antriebstechnik e. V*, Frankfurt a.M.
29. DIN 1342-2:2003-11 (2003) Viskosität – Teil 2: Newtonsche Flüssigkeiten
30. DIN 51563:2011-4 (2011) Prüfung von Mineralölen und verwandten Stoffen – Bestimmung des Viskosität-Temperatur-Verhaltens – Richtungskonstante m
31. Niemann G, Winter H, Höhn B-R, Stahl K (2019) Konstruktion und Berechnung von Verbindungen, Lagern, Wellen. *Maschinenelemente*, vol 5. Springer Vieweg, Berlin, Heidelberg